



## Preparation, Physiochemical and Kinetic Investigations of $V_2O_5/SiO_2$ Catalyst for Sulfuric Acid Production

A. Tavassoli<sup>a</sup>, M. Kazemeini<sup>\*a</sup>, M. Fattahi<sup>b</sup>, L. Vafajoo<sup>c</sup>

<sup>a</sup> Department of Chemical and Petroleum Engineering, Sharif University of Technology, Tehran, Iran

<sup>b</sup> Department of Chemical Engineering, Abadan Faculty of Petroleum Engineering, Petroleum University of Technology (PUT), Abadan, Iran

<sup>c</sup> Faculty of Chemical and Polymer Engineering, Tehran South Branch, Islamic Azad University, Tehran, Iran

### PAPER INFO

#### Paper history:

Received 12 January 2016

Received in revised form 10 September 2016

Accepted 30 September 2016

#### Keywords:

Vanadium Pentoxide

Sulfur Dioxide

Oxidation

Catalyst Preparation

Reaction Kinetics

### ABSTRACT

$V_2O_5/SiO_2$  catalyst was utilized to oxidize  $SO_2$  to  $SO_3$  species in the presence of oxygen mainly for producing sulfuric acid. For this catalyst, the active phase was a mixture of vanadium pentoxide and basic sulfate/pyrosulfate material. This active phase at the reaction temperature behaved as a liquid filling up the pores of the silica support. On the other hand, amounts of the  $SO_3$  and  $V^{5+}$  species in the catalyst necessarily varied with the concentration of the feed material and temperature rendering complexity to the kinetics of the  $SO_2$  oxidation reaction. In the current research, the catalyst preparation with different amounts of such materials was undertaken. Purified diatomaceous earth of a Persian Gulf beach was chosen as the support for this catalyst. The suitability of the prepared catalyst to determine the reaction kinetics was confirmed through the XRD, XRF and BET-BJH analyses as well as color analysis. Moreover, the aforementioned reaction kinetics was studied empirically. In addition, a model for the reaction rate using the response surface methodology (RSM) was presented. In this venue, factors including the reaction temperature as well as conversion were considered. This reaction kinetics determined at the operating conditions of 380-420 °C, 0.108 MPa and feed gas composition of 10 wt.%  $SO_2$ , 18.9 wt.%  $O_2$  and 71.1 wt.%  $N_2$ . It was revealed that, obtained kinetic rate constants satisfied the Arrhenius relationship from which the activation energies were determined.

doi: 10.5829/idosi.ije.2016.29.11b.01

## 1. INTRODUCTION

Catalytic oxidation of  $SO_2$  for producing sulfuric acid is one of the oldest known processes. Sulfuric acid rendered various applications and its amount of consumption is considered as one of the indices of industrialization of a country. This acid is produced from different sulfur compounds acting as the raw materials oxidizing the  $SO_2$  into  $SO_3$  species over vanadium catalysts. Ultimately, the sulfuric acid is produced through hydration of the  $SO_3$  material. The aforementioned oxidation was an exothermic reaction at equilibrium through which the number of moles is reduced. Thus, the reaction performance is a function of operating conditions including; temperature, pressure and feed gas composition. Since this reaction is

exothermic, one method to increase conversion of the  $SO_2$  species is to lower the reaction temperature. Indeed, the catalyst will reduce the reaction temperature through lowering of the required activation energy. In the other words, the reaction temperature is decreased to approximately 400°C or lower for this purpose.

Despite attention paid to this reaction for many years, researchers still work to explain the phenomena taking place including; i) a sharp decrease of catalyst activity at a low sulfur dioxide conversion [1]; ii) a sharp change of the Arrhenius dependence at low temperatures [1] and iii) the activity hysteresis with regards to the conversion and temperature [1]. It is reiterated that, the  $SO_2$  oxidation to  $SO_3$  over vanadium catalysts is accompanied with some other industrial processes such as DeNO<sub>x</sub> with ammonia or regeneration of cracking catalysts [2, 3]. However, the aforementioned phenomena are solely inherent catalysts

\*Corresponding Author's Email: [kazemini@sharif.ir](mailto:kazemini@sharif.ir) (M. Kazemeini)

for the sulfuric acid production. The rationale for this was that, under reaction conditions, the catalyst active components were a melt through bulk of which the reaction took place.

In situ studies focusing on the active component performance, reaction mechanism and catalyst state revealed that, all phenomena understudied were related to the phase transitions of this active material. These involved crystallization of the vanadium (IV) species [1]. Active component melt was represented by the complex of  $M_2S_2O_7$ - $M_2SO_4$ - $V_2O_5$  through which the alkaline admixtures M (M = K, Na, Cs) acted as a promoter. In accordance with the detailed reaction mechanism previously reported [4], the catalytic cycle occurred in the coordination sphere of binuclear complexes of vanadium (V). However, there was a side process yielding reduced vanadium species mostly  $V^{4+}$ .

Vanadium compounds catalysts in the oxidation of the sulfur dioxide are considered to be the most important step in production of the sulfuric acid [5]. Practically, supports with high quality significantly improved the catalyst performance at vanadium catalysts in order to produce the sulfuric acid [6, 7]. Normally, the most common material utilized as a catalyst support is diatomite, a natural clay composed of silica microfossils derived from aquatic unicellular algae comprising of a significant number of diatom units (DU) with various shapes and sizes (10-200  $\mu\text{m}$ ) as well as high porosity (80-90%) [8, 9]. Due to its highly porous structure and low density, diatomite has been widely used as adsorbent, filtration media and support for sulfuric acid production due to the diatomite pores possessing suitable reaction fields for the  $SO_2$  oxidation to  $SO_3$  [10-14]. Besides, this porous support contained longitudinal channels or passage ways permitting the transmission of reactants (e.g.;  $SO_2$  and  $O_2$ ) with minimum pressure drops and high space velocities. Furthermore, the catalyst's effectiveness factor and effective diffusion coefficient for the reaction might be enhanced through improving the support pore size. Small internal pores of the supports lead to insufficient catalyst utilizations as reactants do not have enough time and space to contact with the catalytic components. Moreover, reactants tend to become trapped and participate in undesired secondary reactions [15]. Therefore, diatomite with sufficiently large pores act as a proper support alleviating such problems. On the other hand, due to excessive mining, high-quality diatomites are rather difficult to obtain and most mined ones show an improper pore size distribution (PSD) and high impurity contents. These diatomites are unable to meet the demands of the sulfuric acid industry. Hence, improving the characteristics of diatomite such as the PSD and reducing the impurity content are essential for enhancing the performance of the corresponding catalyst [16]. Until now, several methods have been developed to improve the quality of diatomite [9, 10, 15,

17, 18]. Although these methods remove some of the impurities and slightly improve the PSD, the procedures utilized were relatively complex and the treatment capacity was low. Besides, some of these methods produce unwanted wastes. Therefore, a facile, low-cost, large-scale and environmentally friendly modification approach is needed.

Active component of vanadium catalysts for  $SO_2$  oxidation was proved to be a melt under reaction conditions. This melt consisted of sulfates and pyrosulfates of alkaline metal containing dissolved vanadium complexes. When reaction temperature and  $SO_2$  conversion were low, phase transitions occurred in the melt condition. These transitions were related to the crystallization of compounds of vanadium (IV). The crystal phase formation are usually known to worsen the catalyst activity [1]. Moreover, in a previous research it was shown that, the rate of crystallization process depended upon many parameters including; reaction conditions, active phase chemical composition, support structure and texture as well as the catalyst geometry and prehistory. Crystal phase formation peculiarities and catalyst bed activity changes were well described through the mathematical model based on Gibbs-Folmer theory [1]. In that study, it was revealed that, phase transitions of vanadium (IV) compounds were of reversible character. As temperature or  $SO_3$  concentration increased, the crystal phase fully or partially dissolved and catalyst activity was fully or partially regenerated. In this regard, the crystal phase dissolving peculiarities were of theoretical and practical interest related to the possibility of catalyst activity regeneration [19].

Active phases of catalysts on a silica support surface were generally made of the melted mixture. Moreover, the reaction took place upon this surface under the temperature of 400°C [20, 21]. However, at higher temperatures of 440-600°C, the reaction performed over the active phase was in liquid while at 400-440°C, this reaction took place in an intermediate -state between the liquid and solid [22]. In addition to vanadium, basic metals usually are used as the promoters. Such these metals included Li, Na, K, Rb, Cs for which basic metals with higher molecular weights were preferred. Potassium is a low cost and efficient metal widely utilized in commercial catalysts for the sulfuric acid production. Cesium and Rubidium are more active however; due to high costs they are not as popular. Generally, a considerable part of the reaction is performed on the outer surface or within porosities near surface directly in contact with the gas phase. Hence, catalyst grains with smaller diameters or some possessing higher specific surface areas are preferred to those with larger grains having lower surface to volume ratios. Diameter of the catalyst grains is between 4-10  $\mu\text{m}$  and at most 12  $\mu\text{m}$ . Nonetheless, these were replaced by annular catalysts due to some

hydrodynamic improvements of the latter including; lower pressure drops as well as pore resistivity toward dust blockage compared with other shapes.

In this research, catalyst preparation utilizing different precursor materials were considered. Then, purified diatomaceous earth species from a Persian Gulf beach was chosen as the catalyst support. The suitability of the prepared catalysts for determining the reaction mechanism was confirmed through the characterizations performed including the XRD, XRF, BET-BJH methods as well as the color analysis. Moreover, the prepared materials in this research aimed at investigating the effects of: 1) basic metal silicate (without silicate), 2) addition of vanadium on the specific surface area and the catalyst activity (with vanadium addition), 3) the type of basic metal on the catalyst activity (with only sodium) and 4) the type of basic metals on the catalyst activity (with only potassium). Ultimately, the reaction kinetics of the prepared catalysts were studied with the help of the obtained experimental data.

## 2. CATALYST PREPARATION

General methods of vanadium catalyst preparation were categorized in terms of the order of calcination and shaping steps. Other factors affecting preparation of catalysts included the impregnation solution pH, calcination temperature, sodium precursor utilized, shape of the catalyst as well as the amount of the utilized basic metal silicates in the catalyst [23-27]. Accordingly, an appropriate method of catalyst preparation was chosen and five samples prepared and evaluated. Details of these preparations are provided below.

**2. 1. Preparation of Catalyst Number 1** For this purpose, 29.05 g of sodium silicate was drop-wise added to 20.75 g of solution of 56% KOH. Rigorous mixing of the obtained solution was performed to achieve a homogeneous phase. Then, 6.75 g of  $V_2O_5$  was added under rigorous mixing for 3 h. Next, the obtained solution was filtered. After these steps, 56 mL of 37% sulfuric acid was added to the filtrate solution. By the way, under constant rate the beaker containing this latest solution was quenched in order to prevent gel formation. Finally, 46.05 g Diatomaceous earth soil, whose physical properties are presented in Table 1, was added to the solution and rigorously mixed again. The obtained dough was shaped through an extruder. Pellets of 6 mm in diameter and 6-8 mm in length were the outcome of this shaping process.

Another method of shaping utilized in this work was punching which resulted in a flat surface of the aforementioned dough obtained. Afterwards, the final catalyst for drying was placed in an oven.

**TABLE 1.** Properties of diatomaceous earth utilized

Parameter	Persian Gulf diatomaceous earth
Microscopic structure	Pennate diatom
Initial color	Pinkish white
Total acid-soluble matter (%)	10.65
Water-soluble matter (%)	5
Pore volume before treatment (mL/g)	1.197
Pore volume after treatment (mL/g)	1.56
Color of treated diatomite (with sulfuric acid 20%) after calcination for 3 h at 700°C	White
Color of virgin diatomite after calcination for 3 h at 700°C	Crème
Loss on ignition (LOI) (%) at 960°C for 2h	3.8
Loose density (g/cm <sup>3</sup> )	0.210
Packed density (g/cm <sup>3</sup> )	0.407

Oven temperature increased at a ramp of 1.5 °C/min from the room up to 150 °C and kept there for 10 h. Then, the dried catalysts quenched at a ramp of -1.5 °C/min to the room temperature. Next, the obtained material was heated up from the room temperature up to 600 °C with a ramp of 2.5 °C/min and kept there for 2 h where calcinations occurred. After that, the furnace temperature decreased with a ramp of -2.5 °C/min to the room temperature.

**2. 2. Preparation of Catalyst Number 2** In this method, 30.21 g of 48% KOH was added drop wise to 2.5 g of NaOH. The rigorous mixing of the obtained solution continued till a homogeneous liquid was resulted. Then, 8.01g of the  $V_2O_5$  precursor was added under rigorous mixing for 3 h. Next, the obtained solution was filtered. After these steps, 47.5 mL of 32% sulfuric acid was added to the filtrate solution. By the way, under a constant rate this latest solution was quenched in order to prevent gels formation. Finally, 65.52 g of diatomaceous earth soil was added to this solution under rigorous mixing. The obtained dough was shaped by an extruder. The shaping, drying and calcination process for the prepared material were all previously provided above.

**2. 3. Preparation of Catalyst Number 3** 58.04 g of the sodium silicate was added to 41.51g of the solution of 56% KOH in a drop-wise manner. The well mixing of the obtained solution was performed to obtain a homogeneous liquid phase.

Then, 25.02 g of the  $V_2O_5$  precursor was added under rigorous mixing for 3 h. Next, the obtained solution was filtered. After these steps, 112 mL of 37% sulfuric acid was added to the solution.

By the way, under constant rate the beaker contents were quenched in order to prevent gels formation. Finally, 92.02 g of diatomaceous earth soil was added to the solution and well-mixed. The shaping, drying and calcination steps were the same as those previously described.

**2. 4. Preparation of Catalyst Number 4** In this venue, 29.05 g of sodium silicate was added to 40.42g of solution of 56% NaOH in a drop-wise manner. The well-mixing of the obtained solution was performed till a homogeneous phase resulted. Then, 25.03 g of  $V_2O_5$  was added under rigorous mixing for 3 h. Next, the obtained solution was filtered and 95 mL of 32% sulfuric acid was added to it. By the way, under a constant rate the beaker containing this latest solution was cooled down in order to prevent gels formation. Finally, 112.07 g of diatomaceous earth soil was added to this solution and well-mixed. The shaping, drying and calcination of the prepared catalysts were the same as those previously described.

**2. 5. Preparation of Catalyst Number 5** In this recipe, 41.53 g of solution of 56% KOH was added in a drop-wise manner to 25.03 g of  $V_2O_5$ . The well-mixing of the obtained solution was performed for 3 h to result a homogeneous liquid phase. Next, the obtained solution was filtered and 112 mL of 37% sulfuric acid was added to it. By the way, under a constant rate the beaker contents were cooled down in order to prevent gels formation. Finally, 92.04 g of diatomaceous earth soil was added to the solution and well-mixed. The shaping, drying and calcination of the prepared catalysts were the same as those previously described.

### 3. EXPERIMENTAL RIG

In order to investigate the catalysts performance leading to the reaction kinetic rate expression, a reactor set up was used as presented in Figure 1. The entering feed was a mixture of pure  $SO_2$  and dried air gases with specific ratios controlled by two MFCs. The two aforementioned gases were completely mixed in a tank then entered into a tubular integral reactor placed inside a heating jacket. Through analysis of the feed and exit gases into and from the reactor via the GC method, the respective mole fraction of the  $SO_2$  was determined. Nonetheless, due to rather high costs of this method, Reich-Test utilized. This latter test was to determine the sulfur dioxide content of a gaseous sample through measuring the required volume of the gas needed to decolorize a standard iodine solution. For this purpose, the reaction rate data were obtained at temperatures of 380, 400 and 420 °C and under a pressure of 0.108 MPa utilizing a feed composition of 10 wt%  $SO_2$ , 18.9 wt%  $O_2$  and 71.1 wt%  $N_2$ . These were similar to an industrial

reactor feed for a sulfuric acid plant production. Moreover, it was worth mentioning that, under such conditions, no limiting mass or heat transfer phenomena imposed upon the system. Reaction rate data at the aforementioned temperatures based upon the  $SO_2$  conversion were determined.

### 4. RESULTS AND DISCUSSION

The pictures of the shaped catalyst numbers 1 and 3 are shown in Figures 2 and 3, respectively. The BET-BJH results of the specific surface area and porosity as well as mean pore diameter measurement analysis of these materials are presented in Table 2.

The XRD spectra for the five synthesized catalysts presented in Table 2 are displayed in Figure 4. These confirm the existence of  $V^{4+}$  and  $V^{5+}$  species in the form of  $K_3VO_2(SO_4)_2$  compound which was in agreement with the provided data of another research available in the open literature [28].

Moreover, these results indicated the presence of some amorphous as well as cristobalite structures in the prepared materials. Once again, this latter conclusion was based upon results of another research [29].

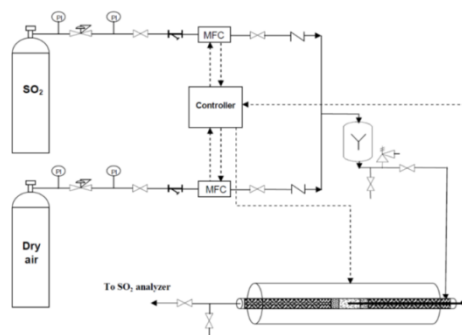


**Figure 1.** Experimental set-up utilized for the sulfur dioxide oxidation reaction in this research (The major elements included  $SO_2$  and dried air capsules, gas mixing tank, mass flow controller, k-type thermocouples, integral reactor and heating jacket)



**Figure 2.** Picture of the extruded form of the catalyst number 1



Figure 3. Picture of punched tablets of the catalyst number 3

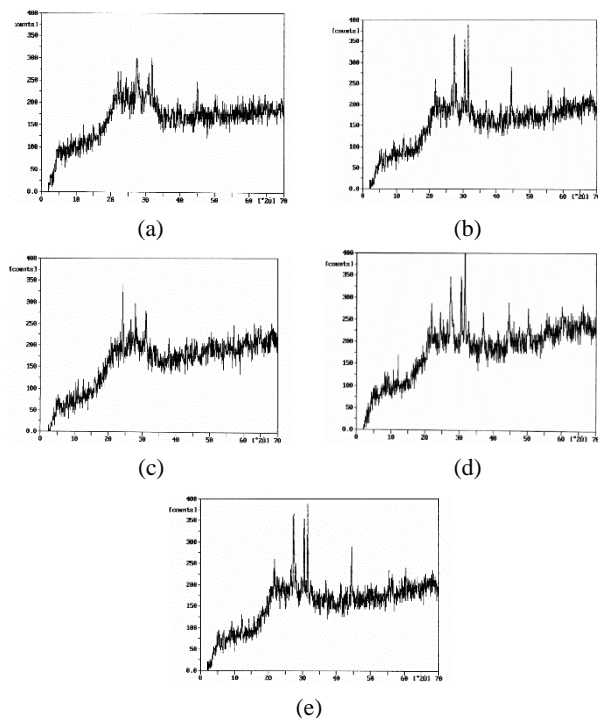


Figure 4. The XRD spectra of the synthesized catalysts: a) No. 1, b) No. 2, c) No. 3, d) No. 4 and e) No. 5 as designated in Table 2

TABLE 2. BET-BJH data of the prepared catalysts

	Specific surface area (m <sup>2</sup> /g)	Mean pore diameter (Å)	Cumulative pore volume (mL/g)
Catalyst No. 1	4.22	38.7	7.1×10 <sup>-3</sup>
Catalyst No. 2	2.16	38.7	4.2×10 <sup>-3</sup>
Catalyst No. 3	2.02	38.7	5.7×10 <sup>-3</sup>
Catalyst No. 4	2.12	33.4	8.7×10 <sup>-3</sup>
Catalyst No. 5	2.00	35.7	6.7×10 <sup>-3</sup>

Although more than 70 years of research has been performed on this catalyst, the details of the catalytic reaction or its kinetics are not understood properly and remained a complex issue. This was due to the fact that, measuring properties of the catalyst's active components at the reaction temperature with characteristics of the melted phase were usually very difficult. In other words, determining such properties at temperatures where the active components still remain solid were not closely related to features of the melted phase. Moreover, besides temperature effects, the catalyst activity is considered as a variable parameter revealing the internal diffusion limitation which often has a pronounced effect upon industrial operating conditions. Therefore, the best route to investigate the process chemical kinetics was measuring the reaction rate directly in the system under industrial operating conditions. To begin with, a reaction rate for kinetic investigations was chosen and a more general equation taking into account the effects of heat and mass transfers were added on. In this venue, there were some basic limitations to relate the micro-structure of the solid and contacting melted layers since introduction of some diffusion and kinetic parameters of very complex nature and practically undeterminable were necessary. Due to these conditions thus, working with such equations was a formidable task. Moreover, there was still a bigger problem associated with this route; there were several possible kinetic equations capable of describing the understudied process. Ultimately, probable reaction rate expressions considered in this research are summarized as follows:

❖ **Power Law Model** This was indeed the simplest applicable form of the rate equation possessing four adjustable parameters provided through the following equation [30]:

$$r = (A P_{O_2}^B P_{SO_2}^C P_{SO_3}^D) F_{eq} \quad (1)$$

In which, A is the pre-exponential factor while B, C and D are the reactants and products exponents of reaction rate and finally,  $F_{eq}$  is the balance factor defined as:

$$F_{eq} = 1 - \frac{P_{SO_3}}{K_p P_{O_2}^{0.5} P_{SO_2}} \quad (2)$$

$K_p$  is a temperature related factor which might have been determined at any given temperature from the following relationship:

$$\log(K_p) = \frac{4956}{T} - 4.678 \quad (3)$$

❖ **Hougen-Watson Model** This model is based on the adsorption-desorption mechanism of reactants and products on the catalyst active sites [31].

$$r = A \frac{P_{SO_2} P_{O_2}^{0.5}}{(B + C P_{O_2}^{0.5} + D P_{SO_2} + E P_{SO_3})^2} F_{eq} \quad (4)$$

This equation was the same as that of the Langmuir-Hinshelwood model multiplied by  $F_{eq}$ . In this equation the parameters of A, B, C, D and E are all adjustable ones.

❖ **Mars-Maessen Model** This equation includes a two-step mechanism namely the i) chemical adsorption of oxygen onto the melted materials and ii) transformation of  $V^{4+}$  to  $V^{5+}$  species; the latter is the rate controlling step [32]. This model possesses two adjustable parameters given by:

$$r = A P_{O_2} \frac{\frac{B P_{SO_2}}{P_{SO_3}}}{\left(1 + \left(\frac{B P_{SO_2}}{P_{SO_3}}\right)^{0.5}\right)^2} \quad (5)$$

❖ **Boreskov Model** This was obtained based on the six-step mechanism in which the oxidation of  $V^{4+}$  to  $V^{5+}$  is the rate determining step [33].

$$r = A \frac{P_{O_2} P_{SO_3}}{P_{SO_2} + B P_{SO_3}} F_{eq} \quad (6)$$

In this relationship, parameters A and B are adjustable.

❖ **Semicek & Kadlec Model** This model provides a four-step mechanism in which the oxidation of  $V^{4+}$  to  $V^{5+}$  species is the reaction rate determining step [34].

$$r = A \frac{\frac{B P_{SO_2}}{P_{SO_3}}}{\left[1 + \left(\frac{B P_{SO_2}}{P_{SO_3}}\right)^{0.5}\right]} \left(P_{O_2} - \frac{P_{SO_3}^2}{K_P^2 P_{SO_2}^2}\right) \quad (7)$$

In this equation, parameters A and B ought to be adjusted.

In order to use any of these models for optimization purposes, the considered objective function to be optimized is taken as follows where N is the number of data points over which calculations are made:

$$O. F. = \frac{\sum_{i=1}^N \left(\frac{r_i^{Calc.} - r_i^{Exp.}}{r_i^{Exp.}}\right)^2}{N} \quad (8)$$

The experimental reaction rates of the first prepared catalyst along with  $SO_2$  conversion are exhibited in Figure 5 at various temperatures. In Figure 5, the amounts of the  $SO_2$  conversion and reaction rate are determined through the following relationships:

$$SO_2 \text{ Conversion (mol. \%)} = \frac{[F_{SO_2}]_{in} - [F_{SO_2}]_{out}}{[F_{SO_2}]_{in}} \times 100 \quad (9)$$

$$(-r_{SO_2}) = \frac{X}{\frac{W}{[F_{SO_2}]_{in}}} \quad (10)$$

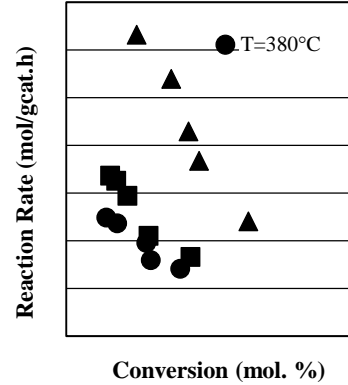


Figure 5. Reaction rate as a function of the  $SO_2$  conversion for the prepared catalyst at different temperatures

where  $F_{SO_2}$  is the molar flowrate of  $SO_2$ , X is the conversion and W is the catalyst weight.

The adjustable parameters of the proposed models (Equations (1) to (7)) were optimized through the MATLAB 7.8 (R2009a) and presented in Table 3. The optimizations were performed at each temperature with the consent that, the results were very sensitive to the initial guesses. In this research, to ensure the accuracy of the results, the developed in-house code was performed with different initial guesses to obtain the lowest error possible for these adjustable parameters. In each model the symbol N presents the number of data points used for the respective error assessment.

A close attention paid to this table revealed that, the power law model optimized the experimental results rather accurately, compared with other considered models. However, the aforementioned model experienced some limitations with prediction of the initial rate of the  $SO_3$  formation due to the power of the  $P_{SO_3}$  term becoming zero or infinity upon the  $SO_3$  formation. Both these situations were indeed irrational. The power of the  $P_{SO_3}$  term at both 380 and 400 °C in the power law model were negative reducing the reaction rate however; at 420 °C these values were positive enhancing such effects on the reaction rate. Nonetheless, these two calculations were not rational. Besides, the  $SO_3$  power varying with the temperature created a difficulty of obtaining a unique reaction rate; the respective kinetic rate constant also did not follow the Arrhenius behavior. Therefore, this model was not a good one from the applicability point of view and discarded from further considerations. The percent error involved was determined through the following relationship:

$$\%E = \frac{\sum_{i=1}^N |r_i^{Exp.} - r_i^{Calc.}|}{N} \times 100 \quad (10-a)$$

The Hougen-Watson model on the other hand, showed an acceptable accuracy toward the experimental data especially under the low temperature regime. Furthermore, the resulting desirable prediction of this model was due to a large number of adjustable parameters of it. The only limitation of this model from application point of view however, was related to the reaction rate kinetic constant A, not obeying the Arrhenius type behavior.

**TABLE 3.** The optimization results of the adjustable model parameters utilized in this research

a) The power law model						
T (°C)	Parameters				%E	
	A	B	C	D		
380	2.303×10 <sup>3</sup>	5.86	-2.07	-0.65	0.0326	
400	2.128×10 <sup>3</sup>	4.16	-0.89	-0.53	0.0445	
420	8.519×10 <sup>4</sup>	2.10	1.12	0.10	0.0553	
b) The Hougen-Watson model						
T (°C)	Parameters					%E
	A	B	C	D	E	
380	54.13	54.01	-176.54	60.97	-64.84	0.0430
400	120.73	45.50	-49.15	49.15	-58.13	0.0564
420	858.88	11.25	-37.77	23.95	-1.03	0.0620
c) The Mars-Maessen model						
T (°C)	Parameters					%E
	A	B				
380	270.4	0.5534				4.08
400	544.64	0.4990				4.56
420	9897.32	0.1731				4.89
d) The Boreskov model						
T (°C)	Parameters				%E	
	A		B			
380	1.8647×10 <sup>18</sup>		0.0222×10 <sup>18</sup>		7.24	
400	1.6552×10 <sup>18</sup>		0.0151×10 <sup>18</sup>		8.36	
420	5.9750×10 <sup>5</sup>		0.0317×10 <sup>5</sup>		10.56	
e) The Semicek & Kadlec model						
T (°C)	Parameters				%E	
	A		B			
380	0.2346		4.3795×10 <sup>4</sup>		4.64	
400	0.2786		5.6692×10 <sup>4</sup>		5.12	
420	28.1585		48.2573		6.10	

In the other words, its dependency on the temperature reached an inflection point. While, at 420 °C this reaction kinetic rate constant reached a maximum, at other considered temperatures a maximum or minimum were observed. Nonetheless, based on the aforementioned limitations obtaining a unique activation energy value despite of low errors of comparison between experimental and predicted data was not possible hence, this model was not chosen as well.

In the Mars-Maessen mechanistic model adding  $P_{SO_2}$  instead of  $P_{SO_3}$  in the model, the limitation of  $P_{SO_3}$  approaching zero was resolved since under such conditions the initial rate approached the  $\frac{A}{B}P_{O_2}$  value indicating that, the initial rate had a pronounced dependency upon the oxygen partial pressure. Nonetheless, this model with the small number of adjustable parameters at low temperatures and conversions showed a good agreement with the experimental results. Besides, the reaction rate kinetic constants followed the Arrhenius behavior and a unique activation energy value was calculated. On the other hand, at the low conversion the agreement of the model with the experimental data was acceptable. This was attributed to the fact that, the derivation of the Mars-Maessen reaction model was far away from the equilibrium condition.

The Boreskov model amongst the undertaken models predicted values with highest deviations from experimental data meaning that, it was eliminated from further considerations.

The Semicek & Kadlec model seemed rather acceptable at investigated temperatures demonstrating low errors. The variation of the reaction rate kinetic constant, A, with the temperature presented an ascending trend. Moreover, the obtained error was a little bit more than that of the Mars-Maessen mechanistic model. However, this model also did not make it as a strong contender since it was not a mechanistic one.

Therefore, it is a foregone conclusion that, the Mars-Maessen model due to the optimum number of parameters, low error analysis and accuracy of the adjustable parameters variations as well as being a mechanistic one was selected as the optimum model in this understudied group of models. Consequently, the reaction rate constant satisfied the Arrhenius behavior very desirably and activation energy of the reaction was obtained to be 40.71kcal/mol (see Figure 6). This value was in the range of values for the catalysts containing potassium and sodium [31, 34]. Furthermore, a rather tight correspondence between results obtained from the Mars-Maessen equation and experimental data reconfirmed that, the SO<sub>2</sub> oxidation obeyed the diffusion and adsorption of the reactants on the melted surface. In the other words, the results of this

mechanistic model revealed that, the understudied catalyst's behavior might not have been described appropriately through a model based on the adsorption-desorption phenomena. Ultimately, the final reaction rate for oxidation of the SO<sub>2</sub> was as follows:

$$\left\{ \begin{array}{l} r = AP_{O_2} \frac{\frac{BP_{SO_2}}{P_{SO_3}}}{\left(1 + \left(\frac{BP_{SO_2}}{P_{SO_3}}\right)^{0.5}\right)^2} \\ A = 2.1925 \times 10^{29} \exp\left(-\frac{40.71}{RT}\right); \quad A = \left[\frac{\text{mol}}{\text{g}_{\text{cat}} \cdot \text{sec} \cdot \text{atm}}\right] \\ B = 0.0205 \exp\left(\frac{15.2311}{RT}\right); \quad R = \left[\frac{\text{kcal}}{\text{mol} \cdot \text{K}}\right] \end{array} \right. \quad (11)$$

In studies where experimental data utilized to determine the kinetic parameters, experimental design might have several benefits due to alleviating time limitations as well as reducing costs and technical considerations. Selection of an appropriate experimental design might therefore be critical to the success of an experimental research. Although non-standard optimal designs were successfully used in previous kinetic studies of heterogeneous catalytic reactions [35, 36], standard designs were not considered as much. Because of the exponential dependence of reaction rates on temperature (*i.e.*; due to the Arrhenius behavior), kinetic rate equations usually exhibited a non-linear behavior. In recent years, applying the standard experimental design of the Response Surface Method (RSM) through its Central Composite Design (CCD) feature has made it possible to use regression tools statistically analyzing a given set of experimental data [36, 37].

The experimental data were analyzed through the RSM using the Design Expert software version 7.0.0 (provided by the Stat-ease Inc., Minneapolis, USA). Its quadratic response surface model was fitted to Equation (12):

$$Y = \beta_0 + \beta_1 X_1 + \beta_2 X_2 + \beta_{11} X_1^2 + \beta_{22} X_2^2 + \beta_{12} X_1 X_2 \quad (12)$$

The predicted response (Y) was therefore correlated to the set of regression coefficients including the; intercept ( $\beta_0$ ), linear ( $\beta_1$ ,  $\beta_2$ ), interaction ( $\beta_{12}$ ) and quadratic ( $\beta_{11}$ ,  $\beta_{22}$ ) coefficients.

All 15 designed experiments and results are depicted in Figure 5. Moreover, the backward regression procedure for the "Design Expert" software was employed to fit the quadratic polynomial Equation (12) to the experimental reaction rate data. The results were analyzed by multiple regression analysis. Consequently, the fitted quadratic model for the SO<sub>2</sub> oxidation reaction was obtained as follows:

$$\begin{aligned} \text{Rate} = & 2693.33007 - \\ & 14.13464 \text{Temperature} + 3.49257 \text{Conversion} + 0.018655 T \\ & \text{emperature}^2 + 2.15711 (13) \times (10)^{-3} \text{Conversion}^2 - \\ & 9.99184 \times (10)^{-3} \text{Temperature} \times \text{Conversion} \end{aligned} \quad (13)$$

In order to determine whether or not the second-order polynomial model (Equation (13)) was significant, it was necessary to conduct an ANOVA analysis. This is

presented in Table 4. These tabulated values indicated that, the quadratic polynomial model was statistically significant ( $P < 0.0001$ ) and adequate to represent the actual relationship between the response (percentile reaction rate) and the significant variables. Furthermore, the coefficient of determination ( $R^2$ ) and the adjusted  $R^2$  of the model were 0.9821 and 0.9731, respectively. These revealed that, the accuracy of the polynomial model was adequate.

Another important statistical item was the coefficient of variation (C.V.) known as the ratio of the standard error of estimate to the mean value of the observed response variable [38]. This also was a measure of reproducibility of the model and as a general rule a model might be considered reasonably reproducible if its C.V. was not greater than 10% [39]. In the present study, a relatively low value of the C.V. (7.76%) indicated a better precision and reliability of the carried out experiments. The level of each variable and the effect of their interactions on the SO<sub>2</sub> oxidation reaction rate were studied by plotting the 3D response surfaces against two independent variables on Figure 7.

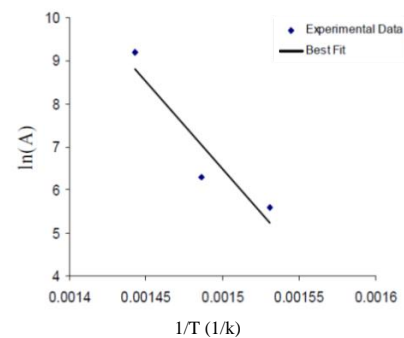


**Figure 6.** Rate constant variations with temperature for determining the activation energy of the SO<sub>2</sub> oxidation reaction performed in this work

**TABLE 4.** Results of regression analysis of CCD experiment

Source	Sum of squares	df	F value	Prob > F
Model	695.09	5	102.12	< 0.0001
A- Temperature	34.88	1	25.62	0.0007
B- Conversion	15.53	1	11.41	0.0082
AB	16.85	1	12.38	0.0065
A2	121.31	1	89.11	< 0.0001
B2	1.13	1	0.83	0.3862
Residual	12.25	9		
Cor Total	707.34	14		
	$R^2=0.9827$	$R^2=0.9731$	C.V.(%)=7.76	

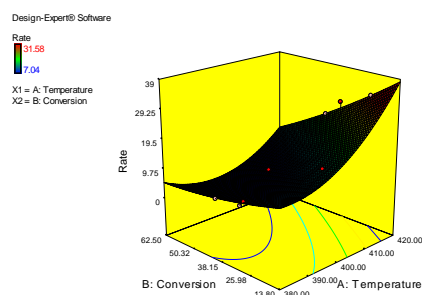


**Figure 7.** Response surface (3-D) methodology showing the effect of reaction temperature and conversion on the  $\text{SO}_2$  oxidation reaction rate

## 5. CONCLUSIONS

In this research, vanadium pentoxide catalyst on silica supports were prepared and utilized to oxidize the reaction of  $\text{SO}_2$  to  $\text{SO}_3$  for the production of sulfuric acid. Active phase of the catalyst was the vanadium species of the  $\text{V}^{5+}$  type and basic metals such as sodium, potassium and cesium were incorporated as promoters onto its structure. Role of the promoters as the activating agents enhanced upon increasing of their atomic weights.

Catalyst active phase at a given reaction temperature was in the form of resolved vanadium in sulfate or pyrosulfate of the basic metal. The respective reaction was performed through diffusing of reactants from the gas to the melted catalyst phase. During this process, initially the  $\text{V}^{5+}$  was reduced to  $\text{V}^{4+}$  species and then the  $\text{V}^{4+}$  material was oxidized back to the  $\text{V}^{5+}$ . Furthermore, several reaction rate models were checked for the five synthesized catalysts against the obtained experimental data and their parameters optimized. Moreover, the RSM based on CCD was employed for modeling and analysis of the  $\text{SO}_2$  oxidation reaction rate.

It was shown that despite the low porosity of the synthesized catalysts, diffusion limitations were not observed for the understudied catalysts. This was indicated through a good fit of the obtained results with the proposed reaction rate expressions. Furthermore, it was revealed that the shape of the prepared catalysts namely, extrudes or punches did not pronouncedly affect the mean pore diameter and PSD of the as-synthesized catalysts. On the other hand, in terms of promoters added, it was shown that, at temperatures below  $420^\circ\text{C}$ , the synthesized catalysts with one promoter did not exhibit any sensible activities. In addition, it was indicated that upon enhancing the amount of vanadium in the catalyst structure to improve its lifetime against poisoning, its specific surface area was initially increased and then upon further enhancement decreased. Thus, there was an optimum amount for the vanadium species for this purpose which

determined to be below 8wt.%. Ultimately, amongst the understudied kinetic models, the best prediction of the obtained experimental data was resulted from the Mars-Maessen which was based on a two-step mechanism (*i.e.*; oxidation-reduction). The activation energy for this model was also determined to be  $40.71\text{ kcal/mol}$ . This was in the range of the reported values for the industrial catalyst using the potassium-sodium basic metals.

This research showed how to synthesize, physiochemically evaluate and determine an optimum kinetic model for a sulfuric acid production catalyst. Ultimately, this type of work might be used as an outline for optimization of a synthesized catalyst or its underlying process towards developing an industrial catalyst.

## 6. REFERENCES

- Bal'zhinimaev, B., Belyaeva, N., Reshetnikov, S., Yudina, E. and Ivanov, A., "Phase transitions in a bed of vanadium catalyst for sulfuric acid production: Experiment and modeling", *Chemical Engineering Journal*, Vol. 84, No. 1, (2001), 31-41.
- Dunn, J. P., Stenger, H. G. and Wachs, I. E., "Oxidation of sulfur dioxide over supported vanadia catalysts: Molecular structure-reactivity relationships and reaction kinetics", *Catalysis Today*, Vol. 51, No. 2, (1999), 301-318.
- Eriksen, K. M., Jensen, C., Rasmussen, S. r. B., Oehlers, C., Bal'zhinimaev, B. and Fehrmann, R., "EPR spectroscopic characterization of  $\text{DeNO}_x$  and  $\text{SO}_2$  oxidation catalysts and model systems", *Catalysis Today*, Vol. 54, No. 4, (1999), 465-472.
- Balzhinimaev, B. S., Ivanov, A. A., Lapina, O. B., Mastikhin, V. M. and Zamaraev, K. I., "Mechanism of sulphur dioxide oxidation over supported vanadium catalysts", *Faraday Discussions of the Chemical Society*, Vol. 87, (1989), 133-147.
- Lozano, L. and Juan, D., "Leaching of vanadium from spent sulphuric acid catalysts", *Minerals Engineering*, Vol. 14, No. 5, (2001), 543-546.
- H. Mahani and M. Kazemeini, "Treatment of diatomaceous earth to obtain its catalyst support", *Scientia Iranica*, Vol. 10, (2003), 350-356.
- Foster, A. I., McCarroll, J. J. and Tension, S. R., "Method for preparing a modified alumina catalyst support and a composition comprising said support and a catalyst", (1980), Google Patents.
- Al-Degs, Y., Khraisheh, M. and Tutunji, M., "Sorption of lead ions on diatomite and manganese oxides modified diatomite", *Water Research*, Vol. 35, No. 15, (2001), 3724-3728.
- Zhang, G., Cai, D., Wang, M., Zhang, C., Zhang, J. and Wu, Z., "Microstructural modification of diatomite by acid treatment, high-speed shear, and ultrasound", *Microporous and Mesoporous Materials*, Vol. 165, (2013), 106-112.
- Li, E., Zeng, X. and Fan, Y., "Removal of chromium ion (III) from aqueous solution by manganese oxide and microemulsion modified diatomite", *Desalination*, Vol. 238, No. 1, (2009), 158-165.
- Kranich Jr, H., "Preparation method for catalyst support and materials produced thereby", (1980), Google Patents.
- Aytas, S. O., Akyil, S., Aslani, M. and Aytekin, U., "Removal of uranium from aqueous solutions by diatomite (kieselguhr)", *Journal of Radioanalytical and Nuclear Chemistry*, Vol. 240, No. 3, (1999), 973-976.

13. Bailey, S. E., Olin, T. J., Bricka, R. M. and Adrian, D. D., "A review of potentially low-cost sorbents for heavy metals", *Water Research*, Vol. 33, No. 11, (1999), 2469-2479.
14. Al-Ghouti, M., Khraisheh, M., Allen, S. and Ahmad, M., "The removal of dyes from textile wastewater: A study of the physical characteristics and adsorption mechanisms of diatomaceous earth", *Journal of Environmental Management*, Vol. 69, No. 3, (2003), 229-238.
15. Wang, D., Niu, T., Straguzzi, G. I., Wright, H. A. and Cnossen, R. G., "Hydrothermal pretreatment for increasing average pore size in a catalyst support", (2005), Google Patents.
16. Yu, J.-S., Kang, S., Yoon, S. B. and Chai, G., "Fabrication of ordered uniform porous carbon networks and their application to a catalyst supporter", *Journal of the American Chemical Society*, Vol. 124, No. 32, (2002), 9382-9383.
17. Al-Wakeel, M. I., "Characterization and process development of the Nile diatomaceous sediment", *International Journal of Mineral Processing*, Vol. 92, No. 3, (2009), 128-136.
18. Wang, M., Xiang, Y., Zhang, G., Song, J., Cai, D. and Wu, Z., "A facile approach to improve the quality of diatomite as sulfuric acid catalyst support", *Applied Catalysis A: General*, Vol. 466, (2013), 185-189.
19. Belyaeva, N., Reshetnikov, S. and Bal'zhinimaev, B., "Phase transitions in the active component of vanadium catalyst for sulfur dioxide oxidation: Crystal phase dissolving", *Chemical Engineering Journal*, Vol. 88, No. 1, (2002), 201-207.
20. Duecker, W. W. and West, J. R., "The manufacture of sulfuric acid", Reinhold Pub. Corp., Vol. 144, (1959).
21. Leach, B., "Applied industrial catalysis, Elsevier, (2012).
22. Simecek, A., "The addition effect of sodium oxide and manganese dioxide on the activity of a vanadium catalyst for sulfur dioxide oxidation", *Journal of Catalysis*, Vol. 18, No. 1, (1970), 83-89.
23. Fennemann, W., Process for producing a V<sub>2</sub>O<sub>5</sub>-and-alkali-metal-sulfate-containing catalyst for oxidizing SO<sub>2</sub> to SO<sub>3</sub>, (1988), Google Patents.
24. Meissen et al., "Production of catalyst for oxidation of SO<sub>2</sub> to SO<sub>3</sub>", United States Patent, No. 4,539,309.
25. Sherif, F. G., "Sulfuric acid catalyst containing vanadium and process therefor", (1978), Google Patents.
26. Hara, H., Kanzaki, T., Motomuro, H. and Adachi, A., "Production of sulfuric acid using a K<sub>2</sub>SO<sub>4</sub>, V<sub>2</sub>O<sub>5</sub>, diatomaceous earth catalyst", (1981), Google Patents.
27. Tavassoli, A., "Preparation and evaluation of vanadium pentoxide for kinetic investigation of sulfur dioxide oxidation in order to sulfuric acid production", M.Sc. Thesis, Sharif University of Technology, (2001).
28. Ksibi, M., Elaloui, E., Houas, A. and Moussa, N., "Diagnosis of deactivation sources for vanadium catalysts used in SO<sub>2</sub> oxidation reaction and optimization of vanadium extraction from deactivated catalysts", *Applied Surface Science*, Vol. 220, No. 1, (2003), 105-112.
29. Jung, K.-W., Jang, D. and Ahn, K.-H., "A novel approach for improvement of purity and porosity in diatomite (diatomaceous earth) by applying an electric field", *International Journal of Mineral Processing*, Vol. 131, (2014), 7-11.
30. Dunn, J. P., Koppula, P. R., Stenger, H. G. and Wachs, I. E., "Oxidation of sulfur dioxide to sulfur trioxide over supported vanadia catalysts", *Applied Catalysis B: Environmental*, Vol. 19, No. 2, (1998), 103-117.
31. Mars, P. and Maessen, J., "The mechanism and the kinetics of sulfur dioxide oxidation on catalysts containing vanadium and alkali oxides", *Journal of Catalysis*, Vol. 10, No. 1, (1968), 1-12.
32. Ivanov, A. A., Borekov, G. K., Buyanov, R. A., Polyakova, G. P., Davydova, L. P. and Kochkina, L. D., "Determination of the kinetic characterization of the oxidation of sulfur dioxide on BAV", *Kinetics and Catalysis*, Vol. 9, (1968), 463-466.
33. Sherif, F. G., "Active and durable sulfuric acid catalyst", (1980), Google Patents.
34. Boghosian, S., Fehrmann, R., Bjerrum, N. and Papatheodorou, G., "Formation of crystalline compounds and catalyst deactivation during SO<sub>2</sub> oxidation in V<sub>2</sub>O<sub>5</sub>-M<sub>2</sub>S<sub>2</sub>O<sub>7</sub> (M= Na, K, Cs) melts", *Journal of Catalysis*, Vol. 119, No. 1, (1989), 121-134.
35. Fattahi, M., Kazemeini, M., Khorasheh, F. and Rashidi, A., "An investigation of the oxidative dehydrogenation of propane kinetics over a vanadium-graphene catalyst aiming at minimizing of the CO species", *Chemical Engineering Journal*, Vol. 250, (2014), 14-24.
36. Fattahi, M., Kazemeini, M., Khorasheh, F. and Rashidi, A. M., "Vanadium pentoxide catalyst over carbon-based nanomaterials for the oxidative dehydrogenation of propane", *Industrial & Engineering Chemistry Research*, Vol. 52, No. 46, (2013), 16128-16141.
37. Fattahi, M., Kazemeini, M., Khorasheh, F. and Rashidi, A., "Kinetic modeling of oxidative dehydrogenation of propane (ODHP) over a vanadium-graphene catalyst: Application of the DOE and ANN methodologies", *Journal of Industrial and Engineering Chemistry*, Vol. 20, No. 4, (2014), 2236-2247.
38. Hajar, M., Shokrollahzadeh, S., Vahabzadeh, F. and Monazzami, A., "Solvent-free methanolysis of canola oil in a packed-bed reactor with use of Novozym 435 plus loofa", *Enzyme and Microbial Technology*, Vol. 45, No. 3, (2009), 188-194.
39. Beg, Q. K., Sahai, V. and Gupta, R., "Statistical media optimization and alkaline protease production from *Bacillus mojavensis* in a bioreactor", *Process Biochemistry*, Vol. 39, No. 2, (2003), 203-209.

# Preparation, Physiochemical and Kinetic Investigations of V<sub>2</sub>O<sub>5</sub>/SiO<sub>2</sub> Catalyst for Sulfuric Acid Production

A. Tavassoli<sup>a</sup>, M. Kazemeini<sup>a</sup>, M. Fattahi<sup>b</sup>, L. Vafajoo<sup>c</sup>

<sup>a</sup> Department of Chemical and Petroleum Engineering, Sharif University of Technology, Tehran, Iran

<sup>b</sup> Department of Chemical Engineering, Abadan Faculty of Petroleum Engineering, Petroleum University of Technology (PUT), Abadan, Iran

<sup>c</sup> Faculty of Chemical and Polymer Engineering, Tehran South Branch, Islamic Azad University, Tehran, Iran

## PAPER INFO

## چکیده

### Paper history:

Received 12 January 2016

Received in revised form 10 September 2016

Accepted 30 September 2016

### Keywords:

Vanadium Pentoxide

Sulfur Dioxide

Oxidation

Catalyst Preparation

Reaction Kinetics

از کاتالیست V<sub>2</sub>O<sub>5</sub>/SiO<sub>2</sub> برای اکسایش SO<sub>2</sub> به SO<sub>3</sub> و در حضور اکسیژن برای تولید اسید سولفوریک استفاده شده است. برای این کاتالیست فاز فعال مخلوطی از پنتاکسید وانادیوم و مواد بازی سولفات/پیروسولفات است. این فاز فعال در دمای واکنش همانند یک مایع که حفرات پایه سیلیکا را پر می‌کنند. از طرف دیگر مقادیر اجزاء SO<sub>3</sub> و V<sup>5+</sup> در کاتالیست با تغییر غلظت خوراک تغییر می‌کند و دما سبب پیچیدگی سینتیک واکنش اکسایش SO<sub>2</sub> می‌شود. در این تحقیق ساخت کاتالیست با مقادیر مختلف بررسی شده است. خاک خالص شده دیاتومی که از سواحل خلیج فارس تهیه شده است. پایداری کاتالیست‌های تهیه شده برای مطالعات سینتیکی با آزمون‌های XRF, XRD و BET-BJH و همچنین آنالیز رنگ تایید شده است. علاوه بر این سینتیک واکنش بدست آماده به صورت تجربی نیز بررسی شده است. همچنین یک مدل سرعت واکنش با استفاده از روش پاسخ سطح (RSM) ارایه شده است. با استفاده از این روش فاکتورهای مورد بررسی شامل دمای واکنش و درصد تبدیل بوده است. سینتیک واکنش در شرایط عملیاتی ۰/۱۰۸ MPa و ۳۸۰-۴۲۰ درجه سانتی گراد ترکیب خوراک ۱۰٪ وزنی SO<sub>2</sub>، ۱۸/۹٪ O<sub>2</sub> و ۷۱/۱٪ N<sub>2</sub> انجام شده است. نتایج نشان می‌دهد که ثابت سرعت سینتیکی بدست آمده منطبق بر رابطه آرنیوس است که انرژی فعال سازی نیز تعیین شده است.

doi: 10.5829/idosi.ije.2016.29.11b.01